Science and Technology for Energy Transition **78**, 43 (2023)

https://doi.org/10.2516/stet/2023028

Available online at:
stet-review.org

REGULAR ARTICLE OPEN ACCESS

Improving the efficiency of solar-driven trigeneration systems using nanofluid coolants★

Bader Alshuraiaan*

Department of Mechanical Engineering, Kuwait University, Jamal Abdul Nasser St, Safat 5969, Kuwait

Received: 28 October 2022 / Accepted: 4 September 2023

Abstract. This article is intended to evaluate methods to improve the efficiency of trigeneration plants, which are designed for the co-generation of heat, electricity, and cold. The possibility of using nanofluids with the addition of oxides of aluminum, silicon, magnesium, and copper, as well as copper itself in the concentration range of 1–6% has been analyzed. The results show that the use of nanofluids can increase the exergic efficiency of the system to 22.9–27.8% and increase thermal efficiency by 23.2–26.7%. It was found that nanofluids have low heat capacity, which may be one of the factors that increase the overall efficiency of trigeneration plants up to 43–60%. Magnesium oxide proved to be the most efficient for generating electricity, with 212.8 kW, aluminum oxide (197.5 kW) for cooling, and copper oxide for generating 98 kW of heat. The Pearson criterion was $\chi^2 = 0.87$, Student's t-test 0.07–0.09, statistical significance of results $p \leq 0.005$.

Keywords: Energy efficiency, Nanofluids, Thermal energy, Solar collector, Trigeneration.

1 Introduction

The use of trigeneration systems has recently been a pressing issue because of the effective use of the recovered energy for heating in winter, air conditioning in summer, and other technological purposes. Most trigeneration systems use fuel to generate heat and produce electricity. Innovative systems use solar collectors [1]. Global electricity production has already exceeded 20 TWh, about 1.5% of which comes from solar power generation [2]. Back in 2010, thermal plants accounted for 80% of the electricity market and used a seventh of the world's freshwater withdrawals [3], whereas in the U.S. and Europe, this value is close to 50% [4]. Especially relevant are trigeneration systems complete with solar collectors in regions with high levels of solar radiation. Cold generation is also an impeccable plus for countries with subtropical and tropical climates [2]. Solar installations can also help reduce toxic emissions associated with thermal power plants [3], which already amount to more than 30 $GtCO_2e$ per year [5]. The authors [6] developed an adsorption chiller with three layers. This chiller with two evaporators produces chilled water with a temperature of about 8 °C and meets the requirements of air conditioning systems. The chiller has a cooling capacity of 100 kW and can be supplied with district heating. The chiller can also be used in seawater or mine water desalination systems [7]. The chiller diagram shown in Figure 1 was tested on a test bench located in the Wroclaw Technology Park. At a water temperature of 62 °C, the chiller achieved a performance coefficient of about 0.7. The maximum efficiency of an adsorption chiller using the water vapor-silica gel system as the working medium is 0.9 [8].

Thus, one can conclude that technologies to convert district heating to cooling with parameters suitable for air conditioning systems have been proven and can be commercialized [9]. These technologies make it possible to realize polygeneration, *i.e.*, simultaneous production of electricity, heat, cold, and other useful products such as desalinated fresh water, technical gases separated from air, or compressed gases. This creates additional opportunities for storing thermal energy after its conversion into cold or other useful products [10]. For example, in Middle Eastern countries, fresh water is a commodity that is always on sale and allows the use of temporary excess heat, including from solar collectors. Despite the maturity of adsorption technologies to realize left-sided thermodynamic cycles with parameters that allow the use of heat systems for air conditioning, adsorption chillers are not widespread. In Kuwait [11], there are several adsorption chillers with heat supply and network heat parameters, but these are research and pilot systems. Given that the efficiency of adsorption chillers is lower than that of electric compressor chillers and that adsorption plants are large and expensive, the rapid

★The proofs have not been corrected by the authors.

* Correspondence: balshuraiaan@outlook.com

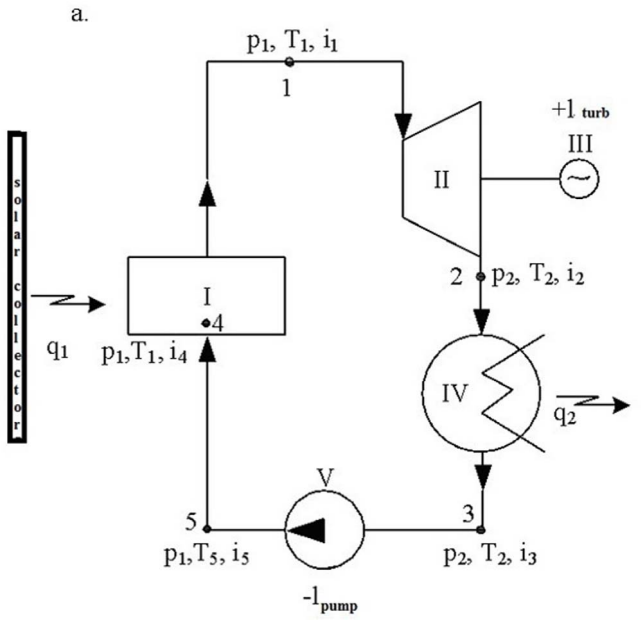

Figure 1. Scheme of trigeneration plant with superheated vapor.

development of trigeneration has economic justification [12]. This situation could change if cogeneration units were to be seen as control generating units of electricity, capable of directly or indirectly using the heat generated using heat storage and trigeneration and poly generation technologies. To summarize, one can state that cogeneration, and in fact, poly generation will play an important role in the transformation of the energy sector [13]. Boiler and polygeneration systems should become flexible power producers and begin to play a regulatory role in the power system, using accumulators of heat, cold, and other products generated by heat consumption from cogeneration. Thanks to advanced technologies for converting heat (including district heating) into cold and technologies for storing heat and cold, cogeneration will be able to meet the needs of the electricity system operator without losing the ability to guarantee the necessary amount of heat and cold [14]. In the new structure of the electric power industry, characterized by a large share of renewable energy sources, cogeneration will replace the unsolved problem of efficient electricity storage with solved problems – the storage of heat, cold, or desalinated water [14].

To make efficient use of low-potential thermal energy, a preliminary scheme of a combined cooling, heating, and power generation system based on metal hydride, operating on solar energy and waste industrial heat, in which both cooling and power generation are achieved, has been proposed [15]. Following a step-by-step procedure recently developed by the authors, two metal hydride pairs were selected for the generation system. The working principle of the system was discussed in detail, and further configuration design for the combined heat and power plant was carried out. Based on the above cycle, energy conversion and exergy analysis models were created [16]. The multi-element method was used to evaluate the performance of the Combined Cooling, Heat, and Power (CCHP) system as a whole, so an analysis of the influencing factors on the system's performance can be done. The typical climatic conditions of Xi'an in 2018 were taken for discussion, and the results showed that the system performance is mainly affected by the amount of solar radiation energy [17]. The system optimization aims to increase the exergy efficiency of the metal hydride heat pump depending on the amount of solar radiation energy. A comparison of two different conventional types of CCHP systems proved that the new CCHP system is superior to conventional CCHP systems in terms of integrated performance [18]. A more realistic theoretical simulation model of tubular solar adsorption cooling is presented (a system using an Activated Carbon-Methanol (AC/M) pair is implemented) [19]. The mathematical model represents the heat and mass transfer inside the adsorption layer [20]. In the cooling cycles of trigeneration plants, the work is done according to the principle of the reverse Carnot cycle. The following types of reverse Carnot cycles are common in industry: cooling, heat pump, and combined processes [11]. The work of the reverse cycle is equal to:

$$l = q_n - q_v \tag{1}$$

where q_v – the heat of the thermal heat source, q_n – the heat of a cold heat source.

$$\varepsilon = \frac{q_n}{l} = \frac{q_n}{q_n - q_o} \tag{2}$$

Cooling factor of the Carnot cycle:

$$\varepsilon_k = T_n/(T_o - T_n) \tag{3}$$

The efficiency of the reverse cycle is estimated by the conversion coefficient θ:

$$\theta = \frac{q_v}{l} = [[q_n/(q_v'' - ''q)]]_o \tag{4}$$

Whereas the conversion factor for the Carnot cycle:

$$\theta_k = \frac{T_v}{T_n[\!['' - T'')]\!]_{''o''}} \tag{5}$$

This scheme is effective for the simultaneous production of heat and cold and is used in trigeneration and cogeneration plants. These units can generate hot water with temperatures up to 70 °C and condition the air up to 8 °C. The disadvantage of this scheme is that the Carnot cycle is difficult to implement under real conditions. The literature also presents the prediction, modeling, and impact of Total Equivalent Warming Impact (TEWI) of a household-sized absorption solar cooling system [20]. The system consists of a solar collector, a storage tank, a boiler, and a LiBr – water-absorbing refrigerator. Experimentally determined heat-mass transfer coefficients were used in the design and cost estimation of a solar-powered cooling machine with a cooling capacity of 11 kW. The solar battery, as found in the simulations, has sufficient capacity to meet the cooling needs of a well-insulated apartment building [21]. The system is simulated with the TRNSYS simulation software using appropriate equations predicting device performance.

Table 1. Physical properties of nanoparticle and base liquid materials [23].

Compound	Density ρ (kg/m^3)	Heat conductivity λ (W/mK)	Heat capacity c_p (kJ/kgK)
Water	1000	0.653	4.22
Al_2O_3	3970	22	0.755
Cu	8920	401	0.385
CuO	6320	77	0.582
MgO	3580	59	0.82
SiO_2	2260	149	0.669

The last optimal system consists of a 15 m^2 composite parabolic collector tilted at an angle of 30° from the horizontal and a 600L hot water storage tank. The total life-cycle cost of a complete system, including the collector and absorption unit, for a lifetime of 20 years would be 13,380 Canadian pounds [22]. Another point contributing to the introduction of innovative thermal energy systems is the trend toward zero-energy buildings. This requires the growing use of renewable energy sources, such as solar energy [23]. In addition, a more efficient use of renewable energy sources is also crucial. However, despite the high prerequisites for the use of trigeneration plants, there are a number of disadvantages, in particular the need to use solid or gaseous fuel. To solve this problem, it is necessary to consider alternative renewable energy sources. The purpose of the work was to investigate the operation of the solar trigeneration system, which uses collectors with nanofluids based on water.

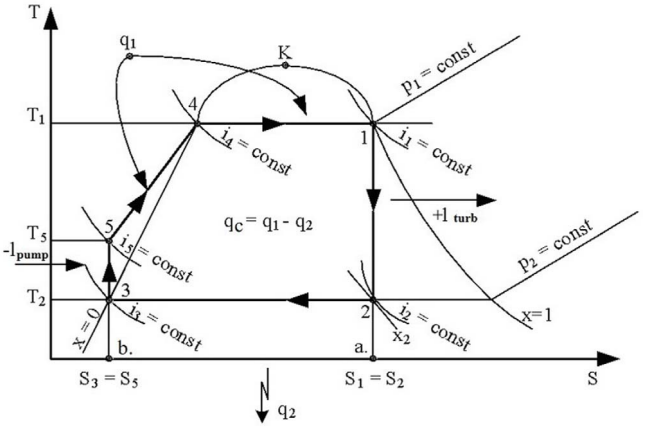

Figure 2. Graphical representation of the cycle in $T = s$-coordinates.

2 Methods

The study of nanofluids' thermophysical properties was carried out in accordance with the method presented by Al-Sulaiman *et al.* [24].

The nanofluid density was determined by the formula:

$$\rho_{\mathrm{nf}} = \rho_{\mathrm{H_2O}}(1-\phi) + \rho_{\mathrm{np}}\phi \tag{6}$$

where ρ_{nf} – nanofluid density; ϕ – volume concentration of nanoparticles in the nanofluid; ρ_{np} – nanoparticle density.

Isobaric heat capacity of nanofluids was calculated by the formula:

$$c_{\rho_{\mathrm{nf}}} = \frac{\rho_{\mathrm{H_2O}}(1-\phi)}{\rho_{\mathrm{nf}}} c_{\rho_{\mathrm{H_2O}}} + \frac{\rho_{\mathrm{np}}\phi}{\rho_{\mathrm{nf}}} c_{\mathrm{p}}\rho_{\mathrm{np}} \tag{7}$$

$c_{\rho_{\mathrm{H_2O}}}$, $c_{\mathrm{p}}\rho_{\mathrm{np}}$, $c_{\rho_{\mathrm{nf}}}$ – isobaric heat capacities of water, nanoparticles, and nanofluid (Tab. 1).

2.1. Thermodynamic calculation of a trigeneration plant using a solar collector

This study tested the operation of a trigeneration system (Fig. 2) including a solar collector. The total capacity of the plant for electricity generation, heating, and cooling was 500 MW. The operation of the trigeneration system was realized using a compensation cycle with superheated vapor. Implementing a refrigeration machine cycle with superheated vapor allows for obtaining more thermal efficiency compared to a cycle without superheated water vapor.

Water ($x_3 = 0$), at temperature T_2 (point 3), is compressed by a pump V (process 3-5) by adiabat at $s_5 = s_3$ = const. At the same time, the water temperature increases (but very slightly) from T_2 to T_5 (points 3 and 5 are very close to each other), and the water pressure at the pump outlet grows from p_2 to p_1. The water from the pump flows into the solar collector and is heated from the temperature T_5 to T_4 – boiling point (process 5-4 – isobaric process at p_1 = const). Water evaporates in the vapor generator (process 4-1 – isobaric-isothermal process of vapor formation at T_1 = const and p_1 = const). This process terminates (in point 1), and the saturated water vapor is fed to the vapor superheater V, where its temperature increases to the temperature T_1 (process 4-1 – isobaric process of superheating vapor at p_1 = const). Superheated dry water vapor is fed to the blades of turbine II, in which the expansion of the vapor takes place (process 1-2 – adiabatic expansion of the vapor, $s_1 = s_2$ = const) with the output of outside work lturb and production of electrical energy in an electric generator III. The temperature of exhaust vapor at the turbine outlet takes the value T_2, pressure – p_2 ($T_2 < T_1$ and $p_2 < p_1$). The degree of vapor dryness is also reduced ($x_2 < 1$) and the vapor becomes wet (point 2 is in the area of wet vapor). Exhaust wet vapor with parameters x_2, i_2, p_2, and T_2 enters the water condenser IV, where it condenses (process 2-3 – isobaric-isothermal process at p_2 = const and T_2 = const). The cycle is completed. In the case of superheated vapor,

its expansion in the turbine (process 1-2) is carried out to pressure p_2, which is below the pressure p_1 and ends in the region of wet vapor (in point 2 $x_2 < 1$). In this case, point 2 is closer to the right boundary curve than in the previous case, i.e., in this process the vapor is dry. Due to this, the turbine operating conditions are easier than in vapor-power plants without vapor overheating and, therefore, the thermal efficiency of the cycle will increase. The amount of heat that is supplied to the working substance to heat it to boiling point (process 4-5) to convert it completely into a vaporous state, and to convert saturated water vapor into superheated one (process 5-1) was calculated as follows:

$$\text{–analytically} : q_1 = i_1 - i_5 \tag{8}$$

$$\text{–graphically} : q_1 = \text{the area under the curve ab541a} \tag{9a}$$

The amount of heat that is removed from the vapor in the condenser by the cooling water (process 2-3 – condensation) was calculated:

$$\text{–analytically} : q_2 = i_2 - i_3$$
$$\text{–graphically} : q_2 = \text{the area under the curve a23ba.} \tag{9b}$$

The thermal efficiency of a trigeneration plant is generally equal to:

$$n_T = \frac{1_c}{q_1} \tag{10}$$

where $1_c = q_1 - q_2$.

By substituting q_1 and q_2 for their calculated values, the following is obtained:

$$n_T = \frac{[(i_1 - i_5) - (i_2 - i_3)]}{(i_1 - i_5)} = \frac{[(i_1 - i_2) - (i_5 - i_3)]}{(i_1 - i_5)} \tag{11}$$

However, $i_1 - i_2 = l_{\text{turb}}$ – (the work that the turbine produces), and $i_5 - i_3 = l_{\text{pump}}$ – (the work expended by the pump). Then:

$$n_T = \frac{[[(1]]_{\text{turb}-1_{\text{pump}})}}{q_1 = 1_c} = \frac{l_c\text{rev}}{q_1} \tag{12}$$

where $l_c$rev – cycle work in reverse process.

Since the work required to compress water is small, one can say that $i_5 - i_3 \sim 0$. Then for approximate calculations, one can use the formula:

$$n_T = \frac{(i_1 - i_2)}{(i_1 - i_5)} = \frac{l_{\text{turb}}}{q_1} \tag{13}$$

It follows that the higher the superheat temperature T_1 and the pressure at which this process takes place (p_1), the higher the thermal efficiency of the Rankine cycle.

Thus, to increase the thermal efficiency of the Rankine cycle, one should try to increase water vapor parameters at the turbine inlet (T_1 and p_1).

2.2. Exergy analysis of a solar trigeneration plant

During the operation of the trigeneration unit, several processes take place, of which the operation of the solar collector, refrigeration unit, and power generation unit are considered. The thermal heat source, as mentioned above is a solar collector, in which nanofluid with parameters p_1 and T_1 circulates as a coolant (working body). The nanofluid flow heats the water in the vapor generator with parameters p_2 and T_2. The resulting vapor does useful work l_{usef}, but in the turbine of the electric generator there is a loss of performance ΔL of the flow:

$$\Delta L = (e_1 - e_2) - l_{\text{usef}} \tag{14}$$

In fact, energy in a trigeneration plant has different values and cannot be infinitely converted from one type to another. Losses are at each stage: energy is irreversibly lost due to irreversible processes, and exergy shows the part of the energy that can be converted into other types, for example, thermal energy is converted into mechanical energy, electrical energy, etc.

Exergy at the inlet to the plant – e_1, and on the output – e_2, and the value (e_1 – e_2) is spent on performing useful work by the system l_{usef} and on the energy. In ideal reversible processes, the loss of performance $\Delta L = 0$, the heat of the nanofluid in the installation could be consumed only to perform work, not to change the internal energy, losses, etc., and the working body in this case performs the maximum useful work:

$$[[L_{(\text{usef}1-2)}]] \max = e_1 - e_2 \tag{15}$$

If the system undergoes an isoentropic change in exergy, the following expression is obtained:

$$\Delta e = e_1 - e_2$$

By substituting this equation into (14), the following is obtained:

$$e_1 - e_2 = i_1 - i_2 + T_o(s_2 - s_1)$$

If the adiabatic process of flowing (working body flow) is reversible, then $s_1 = s_2$ and according to equation (15) the following is obtained:

$$\begin{aligned} e_1 - e_2 &= [[l_{(1-2)}]]\text{rev} \quad \text{that is} \\ e_1 - e_2 &= [[l_{\text{usef}}]] \max . \end{aligned} \tag{16}$$

If the process goes with an increase in entropy, then due to irreversibility, the loss of workability of the flow will be:

$$\Delta L = T_o(s_2 - s_1) \tag{17}$$

The performance loss of the heat flow can also be written as follows:

$$\Delta L = (e_1 - e_2) - l_{\text{usef}} \tag{18}$$

Regardless of the type of process, exergy is the part of the energy that represents the reversibility of processes. Thus, the concept of the exergy of the heat flow is analogous to

the exergy of the working body flow. The exergy of the heat flow is expressed with the following equation:

$$e_q = q\left(1 - \frac{T_1}{T_1}\right) \tag{19}$$

where T_1 and T_2 – temperature at the inlet and outlet of the unit.

Energy losses in thermodynamic cycles can be expressed as a function of heat flow performance loss during the process:

$$\Delta L = \left[\left(e_1 + e_{q_1}\right) - e_2\right] - l_{\text{usef}} \tag{20}$$

where e_1 – the exergy of the working medium inlet flow (vapor, nanofluid, etc.); e_{q_1} – exergy of the input heat flow; e_2 – exergies of all energy flows at the outlet of the trigeneration unit. If the unit operates in isochoric mode and no useful work is performed, the loss of efficiency will be equal to the difference of the exergy at the input and output of the unit.

$$\Delta L = \left(e_1 + e_{q_2}\right) - e_2 \tag{21}$$

The loss of performance ΔL depends also on the operating conditions of the equipment and the thermal insulation of the plant. The share of useful energy (exergy) in the total energy balance of the plant was calculated using the equation (22).

$$n_{\text{ex}} = \frac{l_{\text{effective}}}{e_1 - e_2} \tag{22}$$

The value of the useful work for reversible processes is:

$$l_{\text{usef}} = l_{\text{usef}}^{\max}$$

and

$$l_{\text{usef}\,1-2}^{\max} = e_1 - e_2$$

In this case, the exergy efficiency takes the maximum value

$$n_{\text{ex}} = 1$$

To determine the exergy efficiency of trigeneration plant elements, the following equation was used:

$$n_{\text{ex}} = \frac{e_{\text{out}}}{e_{\text{in}}} \tag{23}$$

2.3. Statistics

To assess the reliability of calculating the energy efficiency of solar collectors for the generation of heat, cold, and electricity in trigeneration plants, it was decided to calculate Student's and Pearson's criteria and the statistical significance of the results according to Alshuraiaan [25].

3 Results

A study of the thermophysical properties of nanofluids used in trigeneration units was conducted. Trigeneration unit parameters obtained experimentally are shown in Figures 3–5.

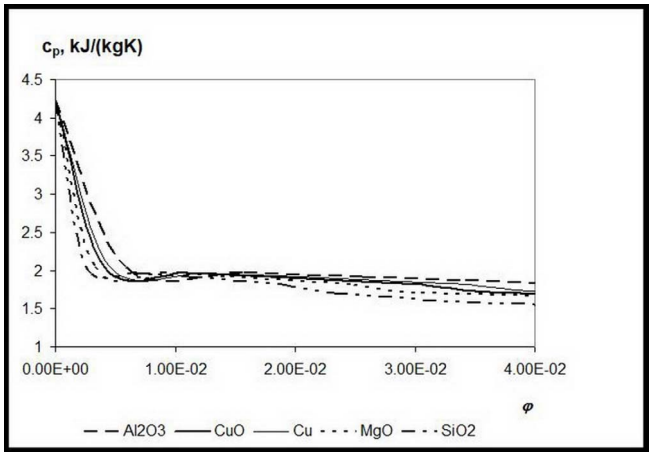

Figure 3. Variation of isobaric heat capacity values of nanofluids depending on nanoparticle concentration.

Isobaric heat capacity was calculated according to (7) and presented in Figure 3.

In the absence of nanoparticles, the highest value of isobaric heat capacity is observed (more than 4 kJ/kgK). As their concentration increases up to 1%, the heat capacity drops sharply to values of 2 kJ/kgK (SiO_2, CuO), 1.9 kJ/kgK (MgO, Cu), 1.82 kJ/kgK (Al_2O_3). A further increase in the number of nanoparticles leads to a smoother decrease in the isobaric heat capacity. At 2% visible differences are observed, the tendency of which is preserved. In the concentration range of 2.0–2.2% SiO_2 the heat capacity decreases by 0.14 kJ/kgK, 2.6–3.0% MgO: by 0.12 kJ/kgK, 3.0–3.6% CuO: by 0.1 kJ/kgK, 3.38–3.88% Cu: by 0.12 kJ/kgK, after which the rate of change of the index decreases. As can be seen from Figure 3, nanofluids tend to decrease isobaric heat capacity, but because their thermal conductivity is higher than that of the base fluid, nanofluids are more efficient heat carriers [25]. Thus, further increasing the number of nanoparticles has almost no effect on the change in thermal conductivity. The nanoparticle concentrations in the nanofluid influenced various system performance indices as well as energy efficiency. The exergy efficiency, calculated according to [26], for nanofluids based on nanoparticles: CuO, Cu, SiO_2, MgO, Al_2O_3, and water, is shown in Figure 4.

The zero concentration of nanoparticles shows the efficiency of the system in pure water. The curves in Figure 4 showed a general tendency for the exergy efficiency to increase with increasing nanoparticle concentration. The presence of 1% of nanoparticles in the liquid leads to a significant increase in the exergy efficiency in the case of all the studied nanoparticles, except SiO_2, where the efficiency increased by only 0.5%, whereas for the other materials, an increase of this index was by more than 1%: MgO: 1.1%, Cu: 2.5%, CuO: 1.7%, Al_2O_3: 4.1%. Finally, the maximum energy efficiency was observed for aluminum oxide: 27.8%. For the other studied oxides, this index was significantly lower, so in the case of SiO_2 it was 22.9%, MgO: 24%, CuO: 25%. For copper particles, the exergic efficiency was

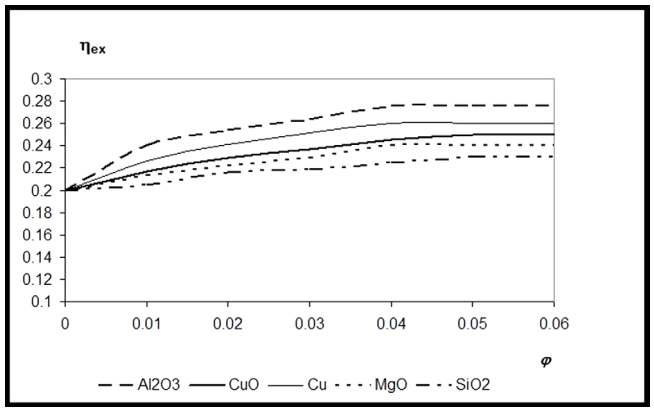

Figure 4. Effect of nanoparticle concentration on the exergy efficiency of the system.

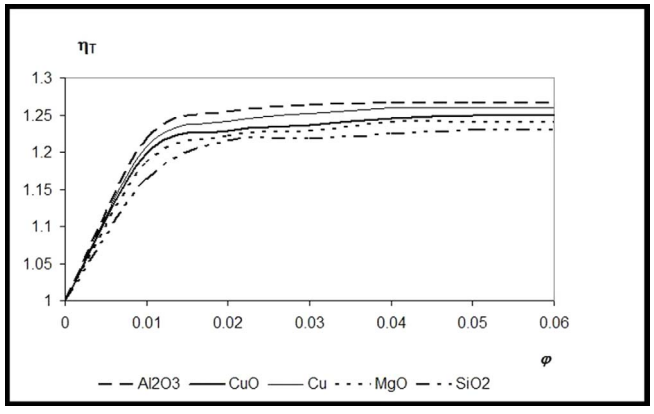

Figure 5. Effect of nanoparticle concentration on the energy efficiency of the system.

26.1%. However, when nanoparticle concentration is higher than 4%, the exergy efficiency practically does not increase $\Delta ex = 0$ –0.0045. It is noteworthy that for all cases with concentrations up to 2% ($\varphi > 0.01$) the use of nanoparticles leads to a dramatic increase in system performance than the pure base liquid, while this trend gradually becomes less pronounced for higher concentrations. Comparing the operation of a trigeneration unit operating with nanofluids ($\varphi > 0$) and pure base fluid (for $\varphi = 0$) shows improvement in all indicators.

Figure 5 shows that the application of nanofluids allows one to increase the productivity of the trigeneration system by up to 25%. The addition of 1% nanoparticles increases the thermal efficiency of the system by 16.3–22.6%. Doubling the concentration of nanoparticles leads to a thermal efficiency increase of 21.3–25.6%. If the liquid contains 3% of nanoparticles, the thermal efficiency increases by 22.2–26.5%, at 4% it increases by 22.8–26.7%, and at 5% it increases by 23.2–26.7%. With further increase, no change in thermal efficiency was observed. In the case of silicon oxide nanoparticles, the thermal efficiency increased by a maximum of 23.2%, and in the concentration range of 1–6% increased by almost 7%. The addition of magnesium oxide particles changed the thermal efficiency by 24.6%, copper oxide by 25%, copper by 26.1%, and aluminum oxide by 26.7%. It should be noted that the maximum increase in thermal efficiency was observed at certain concentrations of particles and did not increase with increasing concentration, namely for SiO_2: 4.8%, MgO: 4.5%, CuO: 5.0%, Cu: 3.9%, Al_2O_3: 3.8%. Regardless of the concentration of particles, the thermal efficiency of the process depends on their nature and increases in the series $SiO_2 < MgO < CuO < Cu < Al_2O_3$. Technical characteristics and results of thermodynamic calculations are presented in Table 2.

From Table 2 it follows that the use of solar collectors on nanofluids in trigeneration plants will increase productivity up to 27.8%. The statistical estimation of the received results has shown sufficient convergence and reliability of experimental results against the theoretical calculations (7–23). The Pearson criterion was $\chi^2 = 0.87$, Student's t-test: 0.07–0.09, and the statistical significance of the results: $p \leq 0.005$.

4 Discussion

The use of a solar collector or solar collector system has undoubted advantages in the heating industry. The developed scheme allows one to create energy installations, which are relevant in regions with a hot climate in terms of air conditioning and the use of solar radiation [27]. Many authors have attempted to produce heat, cold, and electricity using solar panels and solar collectors, but the proposed (in this article) idea of using nanofluid-based solar collectors has significant advantages from a thermodynamic point of view and in terms of cost-effective energy production [28]. For thermodynamic reasons, it is advisable to replace thermal power plants with combined heat and power plants or trigeneration plants [29]. This means that trigeneration will be characterized by increasing dispersion and a tendency to reduce the capacity of electric generators connected to the grid at minimum voltage. The disadvantage of most trigeneration plants is the use of gas or solid-fuel steam generators [16]. More specifically, the heat generated in cogeneration is partially or completely converted into cold in a reverse thermodynamic cycle using a so-called heat pump. Based on the properties of coolants, the implementation of ideal forward or reverse cycles causes certain difficulties. The necessity of heat removal in a heat machine cycle or compression work in a compressor when realizing a refrigeration cycle entails the necessity of heat energy utilization and the selection of equipment for efficient implementation of the processes. Due to the irreversibility of the processes, there are also certain costs. The present study used the Rankine cycle, which is inferior to the Carnot cycle in terms of energy efficiency. However, in ideal processes, for example, there is a problem of wet vapor compression, which in real conditions is unrealistic. The reasons for the impossibility of ideal processes' realization are forces of intermolecular interaction in the working body flow and a very low degree of liquid compression. The way out of this situation is to increase the thermodynamic parameters of the working body in the vapor superheater. Direct conversion of heat into cold is possible

Table 2. Technical characteristics of the solar trigeneration plant.

Parameters	Al_2O_3	CuO	Cu	MgO	SiO_2	χ^2	t
PR_{opt}	0.761	0.849	0.900	0.876	0.87	0.999	0.009
φ_{opt} (%)	4.35	4.64	4.61	5.23	5.3	0.996	0.201
$T_{hr,opt}$ (°C)	113.7	113.7	113.7	113.7	100	0.111	0.008
Exergy efficiency, η_{ex}	0.278	0.25	0.261	0.24	0.229	0.953	0
Energy (thermal) efficiency, η_T	1.267	1.25	1.261	1.246	1.232	0.926	0
Production of electricity, Q_e (kW)	210	202.8	202.3	212.8	210	0.756	0.011
Cold generation, Q_c (kW)	197.5	181	160	136	124	0.023	0.008
Heat production, Q_h (kW)	90	98	77	77	75	0.069	0.002
Solar collector heat, Q_{in} (kW)	500	490	447.9	435.6	415	0.061	0.035
Losses, Q_{loss} (kW)	2.5	8.2	8.6	9.8	6	0.7	0.014
Overall efficiency, η	0.6	0.55	0.44	0.5	0.43	0.869	0

with sorption technologies, while absorption chillers using lithium bromide vapor as the working medium require heat at a temperature no lower than 80 °C, and adsorption chillers using water vapor and silica gel as the working medium can operate from heat at 60–65 °C [17, 26]. The use of solar cooling systems is also a hot topic. In particular, such systems are used for cooling and dehumidifying air in hot and humid regions. The literature mentions a study of the direct cycle in a solar cooling system [11]. Similar results were obtained under subtropical climatic conditions through year-round dynamic modeling of the trigeneration unit using TRNSYS [30]. It was found that the use of a temperature-controlled adsorption cooling cycle in combination with absorption cooling was not a good choice for general applications where controlling the humidity in the working area was not necessary. Some researchers also mention the operating principle of the solar energy recovery plant without heat recovery, which proposes an increase of the solar fraction by 9.5% and a reduction of the total primary energy consumption by 11.5% compared to the previous version, when the seasonal effect was also taken into account. The merits of the proposed solar cooling system with energy recovery increased with the expected improvement in the thermal efficiency of the grid in the long term, confirming the feasibility of the recommended design strategy [30].

5 Conclusion

In the course of the work the possibility of using nanofluids based on aqueous suspensions of Al_2O_3, MgO, CuO, CuO, and SiO_2 in the concentration range of 0–6% was studied. For technical realization, the scheme of the trigeneration unit was used with superheated steam, provided by cycle in T-S coordinates. Comparative analysis showed that the addition of nanoparticles leads to a decrease in the heat capacity of the circulating liquid. Optimal particle concentrations are 4.35% for Al_2O_3, 4.61% for Cu, 4.64% for CuO, 5.23% for MgO, and 5.3% for SiO_2. The exergy and thermal efficiency of the process also increase with any amount of nanoparticles. Thus, the exergic efficiency increased by a value in the range of 2.9–7.8%, while the thermal: 23.2–26.7%. Electricity production by trigeneration system based on the solar panel was the highest in the case of magnesium oxide and was 212.8 kW, heat: in the case of copper oxide (98 kW), and cold: in case of the aluminum oxide (197.5 kW). The total efficiency of the unit was in the range of 43–60%, with the maximum value in the case of aluminum oxide. Pearson criterion was $\chi^2 = 0.67$–0.99, Student's t-test: 1.7·10-7–0.39, and the statistical significance of the results was $p \leq 0.005$. There is a need for further research in this direction using a different composition of nanofluid (changing the qualitative characteristics, using a combination of nanoparticles, or changing their size).

Conflict of interest

The authors declare that the research was conducted in the absence of any commercial or financial relationships that could be construed as a potential conflict of interest.

Funding

This research did not receive any specific grant from funding agencies in the public, commercial, or not-for-profit sectors.

References

1 Kaya I., Colak M., Terzi F. (2019) A comprehensive review of fuzzy multi criteria decision making methodologies for energy policy making, *Energy Strategy Rev.* **24**, 207–228. https://doi.org/10.1016/j.esr.2019.03.003.
2 Nwaigwe K.N., Mutabilwa P., Dintwa E. (2019) An overview of solar power (PV systems) integration into electricity grids, *Mater. Sci. Energy Technol.* **2**, 3, 629–633. https://doi.org/10.1016/j.mset.2019.07.002.
3 Shahzad M.W., Burhan M., Ang L., Ng K.C. (2017) Energy-water-environment nexus underpinning future desalination sustainability, *Desalination* **413**, 52–64. https://doi.org/10.1016/j.desal.2017.03.009.

4 Wang W., Shi Y., Zhang C., Hong S., Shi L., Chang J., Li R., Jin Y., Ong C., Zhuo S., Wang P. (2019) Simultaneous production of fresh water and electricity via multistage solar photovoltaic membrane distillation, *Nat. Commun.* **10**, 1, 3012. https://doi.org/10.1038/s41467-019-10817-6.

5 Scarlat N., Prussi M., Padella M. (2022) Quantification of the carbon intensity of electricity produced and used in Europe, *Appl. Energy* **305**, 117901. https://doi.org/10.1016/j.apenergy.2021.117901.

6 Liu Z., An G., Xia X., Wu S., Li S., Wang L. (2021) The potential use of metal–organic framework/ammonia working pairs in adsorption chillers, *J. Mater. Chem. A.* **9**, 6188–6195. https://doi.org/10.1039/D1TA00255D.

7 Demir M.E., Dincer I. (2021) Development and assessment of a solar driven trigeneration system with storage for electricity, ammonia and fresh water production, *Energy Convers. Manag.* **245**, 114585. https://doi.org/10.1016/j.enconman.2021.114585.

8 El Fil B., Garimella S. (2022) Energy-efficient gas-fired tumble dryer with adsorption thermal storage, *Energy* **239**, 121708. https://doi.org/10.1016/j.energy.2021.121708.

9 Paredes-Sánchez B.M., Paredes J.P., Caparrini N., Rivo-López E. (2021) Analysis of district heating and cooling energy systems in Spain: resources, technology and management, *Sustainability* **13**, 5442. https://doi.org/10.3390/su13105442.

10 Liu Y., Hu X., Luo X., Zhou Y., Wang D., Farah S. (2020) Identifying the most significant input parameters for predicting district heating load using an association rule algorithm, *J. Clean Prod.* **275**, 122984. https://doi.org/10.1016/j.jclepro.2020.122984.

11 Gładysz P., Sowiżdżał A., Miecznik M., Pająk L. (2020) Carbon dioxide-enhanced geothermal systems for heat and electricity production: energy and economic analyses for central Poland, *Energy Convers. Manag.* **220**, 113142. https://doi.org/10.1016/j.enconman.2020.113142.

12 Dabwan Y.N., Pei G., Gao G., Feng J., Li J. (2020) A novel integrated solar tri-generation system for cooling, freshwater and electricity production purpose: energy, economic and environmental performance analysis, *Sol. Energy* **198**, 139–50. https://doi.org/10.1016/j.solener.2020.01.043.

13 Bellos E., Tzivanidis C. (2020) Concentrating solar collectors for a trigeneration system – a comparative study, *Appl. Sci.* **10**, 4492. https://doi.org/10.3390/app10134492.

14 Jafary S., Khalilarya S., Shawabkeh A., Wae-hayee M., Hashemian M. (2021) A complete energetic and exergetic analysis of a solar powered trigeneration system with two novel organic Rankine cycle (ORC) configurations, *J. Clean Prod.* **281**, 124552. https://doi.org/10.1016/j.jclepro.2020.124552.

15 Chen Y., Zhao D., Xu J., Wang J., Lund P.D. (2021) Performance analysis and exergo-economic optimization of a solar-driven adjustable tri-generation system, *Energy Convers. Manag.* **233**, 113873. https://doi.org/10.1016/j.enconman.2021.113873.

16 Sebastián A., Abbas R., Valdés M., Rovira A. (2021) Modular micro-trigeneration system for a novel rotatory solar Fresnel collector: a design space analysis, *Energy Convers. Manag.* **227**, 113599. https://doi.org/10.1016/j.enconman.2020.113599.

17 Li Z., Chen H., Xu Y., Ooi K.T. (2020) Comprehensive evaluation of low-grade solar trigeneration system by photovoltaic-thermal collectors, *Energy Convers. Manag.* **215**, 112895. https://doi.org/10.1016/j.enconman.2020.112895.

18 Meng X., Yang F., Bao Z., Deng J., Serge N.N., Zhang Z. (2010) Theoretical study of a novel solar trigeneration system based on metal hydrides, *Appl. Energy* **87**, 2050–2061. https://doi.org/10.1016/j.apenergy.2009.11.023.

19 Hassan H.Z., Mohamad A.A., Bennacer R. (2011) Simulation of an adsorption solar cooling system, *Energy* **36**, 530–537. https://doi.org/10.1016/j.energy.2010.10.011.

20 Florides G.A., Kalogirou S.A., Tassou S.A., Wrobel L.C. (2002) Modelling, simulation and warming impact assessment of a domestic-size absorption solar cooling system, *Appl. Therm. Eng.* **22**, 1313–25. https://doi.org/10.1016/S1359-4311(02)00054-6.

21 Calise F., Cappiello F.L., d'Accadia M.D., Vicidomini M. (2020) Energy and economic analysis of a small hybrid solar-geothermal trigeneration system: a dynamic approach, *Energy* **208**, 118295. https://doi.org/10.1016/j.energy.2020.118295.

22 Sabadash V., Gumnitsky J., Lyuta O. (2020) Combined adsorption of the copper and chromium cations by clinoptilolite of the sokyrnytsya deposit, *J. Ecol. Eng.* **21**, 42–46. https://doi.org/10.12911/22998993/122185.

23 Fong K.F., Lee C.K. (2020) Solar desiccant cooling system for hot and humid region – a new perspective and investigation, *Sol. Energy* **195**, 677–684. https://doi.org/10.1016/j.solener.2019.12.009.

24 Al-Sulaiman F.A., Dincer I., Hamdullahpur F. (2011) Exergy modeling of a new solar driven trigeneration system, *Sol. Energy* **85**, 2228–2243. https://doi.org/10.1016/j.solener.2011.06.009.

25 Alshuraiaan B. (2021) Evaluation of the thermal performance of various nanofluids used to harvest solar energy, *Energy Ecol. Environ.* **6**, 531–539. https://doi.org/10.1007/s40974-021-00213-6.

26 Ealia S.A.M., Saravanakumar M.P. (2017) A review on the classification, characterisation, synthesis of nanoparticles and their application, in: *IOP Conference Series: Materials Science and Engineering*, Vol. **263**, IOP Publishing, Bristol, p. 032019. https://doi.org/10.1088/1757-899X/263/3/032019.

27 Jiang Y., Zhang H., Wang Y., You S., Wu Z., Fan M., Wang L., Wei S. (2021) A comparative study on the performance of a novel triangular solar air collector with tilted transparent cover plate, *Sol. Energy* **227**, 224–235. https://doi.org/10.1016/j.solener.2021.08.083.

28 Calise F., Cappiello F.L., d'Accadia M.D., Vicidomini M. (2021) Thermo-economic optimization of a novel hybrid renewable trigeneration plant, *Renew. Energy* **175**, 532–549. https://doi.org/10.1016/j.renene.2021.04.069.

29 Eguchi S., Takayabu H., Lin C. (2021) Sources of inefficient power generation by coal-fired thermal power plants in China: a metafrontier DEA decomposition approach, *Renew. Sustain. Energy Rev.* **138**, 110562. https://doi.org/10.1016/j.rser.2020.110562.

30 Gholizadeh T., Vajdi M., Rostamzadeh H. (2020) A new trigeneration system for power, cooling, and freshwater production driven by a flash-binary geothermal heat source, *Renew. Energy* **148**, 31–43. https://doi.org/10.1016/j.renene.2019.11.154.